PLOS ONE

RESEARCH ARTICLE

Ultrasonic cavitation induces necrosis and impairs growth in three-dimensional models of pancreatic ductal adenocarcinoma

Einas Abou Ali[1,2], Benoit Bordacahar[1,2], Jean-Louis Mestas[3], Frederic Batteux[2,4], Cyril Lafon[3], Marine Camus[1,2,4], Frederic Prat[1,2,4]*

1 Cochin Hospital, Gastroenterology and Endoscopy Department, Paris, France, **2** Cochin Institute, Paris, France, **3** Inserm, U1032, LabTau, Lyon, France; Université de Lyon, Lyon, France, **4** Paris Descartes University, Paris, France

* frederic.prat@aphp.fr

OPEN ACCESS

Citation: Abou Ali E, Bordacahar B, Mestas J-L, Batteux F, Lafon C, Camus M, et al. (2018) Ultrasonic cavitation induces necrosis and impairs growth in three-dimensional models of pancreatic ductal adenocarcinoma. PLoS ONE 13(12): e0209094. https://doi.org/10.1371/journal.pone.0209094

Editor: Aamir Ahmad, University of South Alabama Mitchell Cancer Institute, UNITED STATES

Received: July 21, 2018

Accepted: November 28, 2018

Published: December 31, 2018

Data Availability Statement: All data is shared on https://datadryad.org/review?doi=doi:10.5061/dryad.3hf5gb3.

Funding: The authors received no specific funding for this work.

Competing interests: The authors have declared that no competing interests exist.

Abbreviations: 3D, three dimensional; CI, Cavitation Index; Gem 5 μM, Gemcitabine at a

Abstract

Introduction

Pancreatic ductal adenocarcinoma (PDAC) is a rapidly increasing cause of mortality whose dismal prognosis is mainly due to overwhelming chemoresistance. New therapeutic approaches include physical agents such as ultrasonic cavitation, but clinical applications require further insights in the mechanisms of cytotoxicity. 3-D in vitro culture models such as spheroids exploit realistic spatial, biochemical and cellular heterogeneity that may bridge some of the experimental gap between conventional in vitro and in vivo experiments.

Purpose

To assess the feasibility and efficiency of inertial cavitation associated or not with chemotherapy, in a spheroid model of PDAC.

Methods

We used DT66066 cells, derived from a genetically-engineered murine PDAC, isolated from KPC-transgenic mice (LSL-Kras$^{G12D/+;}$ LSL-Trp53$^{R172H/+;}$ Pdx-1- Cre). Spheroids were obtained by either a standard centrifugation-based method, or by using a magnetic nano-shuttle method allowing the formation of spheroids within 24 hours and facilitating their handling. The spheroids were exposed to ultrasonic inertial cavitation in a specially designed setup. Eight or nine spheroids were analyzed for each of 4 conditions: control, gemcitabine alone, US cavitation alone, US cavitation + gemcitabine. Five US inertial cavitation indexes, corresponding to increased US intensities, were evaluated. The effectiveness of treatment was assessed after 24 hours with the following criteria: spheroid size (growth), ratio of phase S-entered cells (proliferation), proportion of cells in apoptosis or necrosis (mortality). These parameters were assessed by quantitative immunofluorescence techniques.

concentration of 5 μM; NS, nano shuttle; NS+ cell, cell incubated with NS; US, ultra sound.

Results

The 3D culture model presented excellent reproducibility. Cavitation induced a significant decrease in the size of spheroids, an effect significantly correlated to an increasing cavitation index ($p < 0.0001$). The treatment induced cell death whose predominant mechanism was necrosis ($p < 0.0001$). There was a tendency to a synergistic effect of US cavitation and gemcitabine at 5μM concentration, however significant in only one of the cavitation indexes used ($p = 0.013$).

Conclusion

Ultrasonic inertial cavitation induced a significant reduction of tumor growth in a spheroid model of PDAC., with necrosis rather than apoptosis as a Cell dominant mechanism of cell death. More investigations are needed to understand the potential role of inertial cavitation in overcoming chemoresistance.

Introduction

Pancreatic ductal adenocarcinoma (PDAC), a currently leading cause of cancer mortality, has a rapidly increasing incidence and is expected to become the second cause of cancer death within 10–15 years [1]. The overall 5-year survival rate of PDAC does not exceed 8% [2]. Only 20% of patients have a resectable disease at diagnosis, and the 5-year survival rate in this surgical subgroup does not exceed 20%, as a result of early local and metastatic tumour spread as well as chemoresistance [3]. Even recent innovative combined chemotherapy regimens like Nab-pacitaxel + Gemcitabine [4], and FOLFIRINOX [5] have only marginally improved the median overall survival of non resectable pancreatic cancer and the surgical resection rates after neoadjuvant chemotherapy or chemo-radiation [6]. A major limitation in effectively treating PDAC using conventional and targeted chemotherapeutic agents is inadequate drug delivery to the target location, predominantly due to a poorly vascularized, desmoplastic tumor microenvironment, whose mass is predominant in PDAC [7].

Therapeutic focused ultrasound has been shown to have its own anti-tumoral effect, and also to improve drug delivery, in both *in vitro* and *in vivo* models of different types of [8–13]. Ultrasound can induce tumor cell death by focal heating (HIFU) or by the initiation, growth, oscillation and collapse of gas bubbles (cavitation). Cavitation creates tensile acoustic pressures larger than cohesion forces between molecules and thus enhances the penetration of drugs (steady cavitation) or creates irreversible damage to membranes and extracellular matrix (inertial cavitation). The physical properties of inertial cavitation make it likely to bear the most promising potential to overcome the barriers of PDAC microenvironment because disrupting the microenvironment in which PDAC cells are encased is considered a prerequisite to allow chemotherapy to penetrate membranes and induce tumor cell death. However, although some interesting results have been obtained by our group as well as others [13–15], and *Camus M. et al*, *COCHIN Institute*, *submitted*,] small animal experiments have neither helped understand the mechanisms of cell death under ultrasonic cavitation nor optimize the combination of ultrasound and chemotherapy, a reason among others being that animal models do not offer sufficient reproducibility in terms of growth and response to draw robust conclusions.

To establish a tissue culture model simulating complex three-dimensional intercellular interactions, we worked on a model of multicellular spheroids of genetically engineered

murine PDAC, including a three-dimensional (3D) cell culturing system based on magnetic bioprinting [16–17]. This model can help apprehend the effects of cavitation on cells and extracellular components of the microenvironment. In this first study, we aimed to evaluate the effects sustained by PDAC spheroids after exposure to inertial cavitation in the presence or absence of chemotherapy.

Material and methods

Cell culture

DT66066 cells were isolated from KPC-transgenic mice (K-ras$^{LSL.G12D/+}$; p53$^{R172H/+}$; PdxCre) [18–19]. DT66066 cells were cultured in Dulbecco's Modified Eagle's Medium (DMEM, Thermo Fischer Scientific, USA). Media were supplemented with 10% Fetal Bovine Serum (Thermo Fischer Scientific, USA), 1% penicillin G-streptomycin (Thermo Fischer Scientific, USA) and 1% ciprofloxacin (Ciflox, Bayer), and replaced every 3 days. Cells were cultured at 37˚C with 5% CO_2. At 80% confluency, the cells were detached with 0.25% trypsin for subculturing.

"Nano-shuttle spheroids" by magnetic cell bioprinting

Three-dimensional bioprinting cell cultures were based on previously established methodology [16] and were set up using the 24-well Bio-Assembler kit (Nano3D Biosciences, Inc.) consisting of nano-shuttle (NS) solution and a 24-well plate magnetic drive. The NS is a nanoparticle assembly of iron oxide (Fe_2O_3) and gold (Au) nanoparticles cross-linked with poly-l-lysine to promote cellular uptake. The 24-well plates used for 3D culture were flat bottom ultra-low attachment plates.

At 80% confluency in a cell culture flask (25cm^2, 75cm^3, Thermo Fischer Scientific, USA) cells were mixed with 8μL of NS per cm2 plate area and placed in a standard CO_2 cell culture incubator (37˚C, 5% CO_2 in air) for 12 hours in standard adherent culture conditions. Cells were then trypsinized to detach adherent cells from plate and to obtain single-cell suspension. After trypsin inactivation with serum, cells were counted, centrifuged, and seeded into a multi-well ultralow-attachment plate. The medium volume in each well was 0.4ml (cell concentration: 2.5 X 10^5 cell per mL) for the 24-well plate. A magnetic drive was immediately placed under the culture to magnetically bioprint the cells and guide them to aggregate within hours. The cells aggregated just above each magnet, at the center of the well, where they self-assembled into a spheroid. Bioprinted spheroids were incubated in a CO_2 incubator, and the magnetic drive was removed after 24 hours of incubation.

Because 3D cultures are magnetized, the same magnet drive was used to facilitate medium exchange throughout the 3D cell culturing process, and spheroid handling was achieved with a magnetic pen.

Validation of nano-shuttle biocompatibility

Nano-shuttle is a nanoparticle assembly (~ 50 nm) consisting of gold, iron oxide, and poly-L-lysine (PLL), that attaches to the plasma membrane electrostatically. NS are then incorporated into cell cytoplasm, and released off the cell into the surrounding extracellular matrix over 16 hours for 2D cultures, and over 8 days for 3D cultures, [16–17].

Several publications have used 3D culturing cells based on NS with different cell lines, [14,17–23] and confirmed its biocompatibility. In particular these publications demonstrated that NS did not affect cell proliferation [20,21], viability [21], metabolism [20,22], inflammatory stress [20], or phenotype [16,20,22]. decided to investigate NS biocompatibility using

DT66066 cells, and to evaluate the potential effect of these NS on chemotherapy and ultrasound cavitation cell sensitivity.

A transmission electron microscopy was performed to assess any cell architectural abnormality after 12 hours of incubation with NS. Cell proliferation, oxidative stress, gemcitabine cell sensitivity, and ultrasound cell sensitivity were studied with and without cell incubation with NS (12 hours of incubation).

These experiments were performed using samples of DT66066 cell suspension (for proliferation and chemosensitivity after incubation with NS: cell concentration was 10^4 cell/ml in 200 mL of media per well for each sample; for the NS and cell sensitivity to US experiment, (including also NS and oxidative stress experiment) we used 10^5 cells/ml in 600mL of media in a 2ml Eppendorf sterile tube for each sample).

Ultrasound cavitation and chemotherapy treatments

The ultrasonic setup used has been previously described by Chettab et al. [23], but adjusted in our study to generate inertial cavitation instead of stable cavitation.

Briefly, it is composed of two piezo-ceramic focused transducers of 50 mm diameter, 50mm curvature, and F = 1.1 MHz frequency. These are separated by an angle of 90˚ and placed in order to match their respective focal points. An in-house hydrophone is placed in the water tank to record acoustic cavitation emissions from the focal area. The excitatory signal is generated by a waveform generator (PXI 5412 National Instruments, Austin,TX) and amplified with a 200 W power amplifier (LA200H, Kalmus, Bothell, WA). This signal is a burst of 2750 sinusoidal cycles with frequency of 1.1 MHz and a repetition frequency of 100 Hz, mostly generating an inertial cavitation regimen. The setup was filled with Ablasonic (EDAP-TMS, France), a cavitation-inhibiting fluid, preventing acoustic cavitation occurrence outside the sample submitted to ultrasound.

Each spheroid was individually placed in an 2ml sterile Eppendorf tube (Eppendorf, Germany), and placed in the center of the setup, so that the spheroid was inevitably in the focal point. Several inertial cavitation index (CI) were tested (CI 10, CI 14, CI 18, CI 22 et CI 26, during 20 seconds), corresponding to crescent US intensities.

A pre-treatment with gemcitabine at a concentration of 5 μM was performed during 4 h before the US application in designated spheroid groups. The other groups of spheroids included three conditions: no-treatment, US treatment only, gemcitabine treatment only. Spheroids were then replaced in their initial media (i.e. with or without gemcitabine) and incubated during 24 hours.

Evaluation of cell proliferation, and oxidative stress

The UptiBlue Viable Cell Counting assay was used to measure quantitatively the proliferation.

Intra-cellular oxidative stress was evaluated by glutathione and H2O2 measurement using a spectrofluorimeter (Fusion microplate reader fluorometer, Packard).

Cell viability, glutathione and H2O2 measurement were calculated using the GraphPad Prism 5.0 software (GraphPad Software Inc., San Diego, CA) was expressed relative to untreated control.

Immunofluorescence evaluation of US cavitation +/- chemotherapy treatment efficiency

Three end-points were evaluated: proliferation, apoptosis and necrosis.

Cell proliferation was quantified using the Click-it EdU Assay (Alexa fluor 488, Invitrogen, Life Technologies, USA). This assay is an alternative to the BrdU assay. EdU (5-ethynyl-2′-

deoxyuridine) provided in the kit is an analog of thymidine and is incorporated into DNA during active DNA synthesis. A concomitant labeling of spheroids by DAPI (DAPI nucleic acid stain, Invitrogen, Life Technologies, USA) fluorescence was performed.

Apoptosis and necrosis were quantified using respectively YO-PRO-1 (YO-PRO-1 (491/509), Invitrogen, Life Technologies, USA) and Propidium iodide (Propidium Iodide (535/617), Invitrogen, Life Technologies, USA) labeling.

Images acquisition and analysis

Transmission electron microscopy (TEM) was performed with a Jeol transmission electron microscope (Jeol TEM, USA).

Fluorescence images from spheroids were acquired using a straight confocal microscope, SPINNING DISK Leica DM6000 (Leica, Germany), using a 25X objective. Images were processed using Metamorph (Molecular Devices, USA) and ImageJ (ImageJ software, W.Rasband, NIH, USA) softwares.

The size of spheroids was estimated by measuring the largest diameter. Measuring Cell Fluorescence using ImageJ, was fulfilled by a method previously described [24,25] based on the following formula:

Corrected Total Cell Fluorescence (CTCF) = Integrated Density–(Area of selected cell X Mean fluorescence of background readings)

Statistical analysis

Data are presented as mean ± standard deviation (SD). An ANOVA test was performed considering the number of conditions studied (more than 2). Mann-Whitney test was used for pharmacokinetic results (i.e validation of nanoparticles biocompatility). Statistical analyses were performed by Graphpad Prism software (GraphPad Software, Inc., La Jolla, California, USA). Results were considered to be statistically significant for a p value <0.05.

Results

Validation of nano-shuttle (NS) biocompatibility

Fig 1 shows a transmission electron microscopy acquisition of DT66066 cells after 12 hours of incubation with NS. NS are incorporated into cell cytoplasm inside endocytic vacuoles. No NS were detected into cell nuclei, and no architectural abnormalities were identified.

For each condition, 17–20 samples were analyzed. NS affected neither cell viability, proliferation, or chemosensitivity under gemcitabine exposure (Fig 2).

For each condition, 6 samples were analyzed (total 84 samples). NS potentiated ultrasound cell sensitivity at highest levels of cavitation index—CI 16, CI18 and CI 20 (respectively $p = 0{,}0024$, $p = 0{,}0417$, $p<0{,}0001$)—as shown by a reduction of cell proliferation for the DT66066 cells incubated with NS (NS+) (Fig 3), but not at lower CI indexes.

For each condition 6 samples were analyzed (a total of 84 samples for glutathione experiments and 84 other samples for H_2O_2 experiments). NS did not affect oxidative stress for most cavitation indexes. Glutathione and H_2O_2 levels were only significantly elevated for NS+ cells when treated with the highest cavitation index tested, i.e. CI 20 (respectively $p<0{,}0001$, $p = 0{,}0088$) (Fig 4).

US cavitation treatment

At 72 hours of growth, spheroids were treated with increasing US inertial cavitation index, preceded or not by a 4 hours 5 μM gemcitabine incubation.

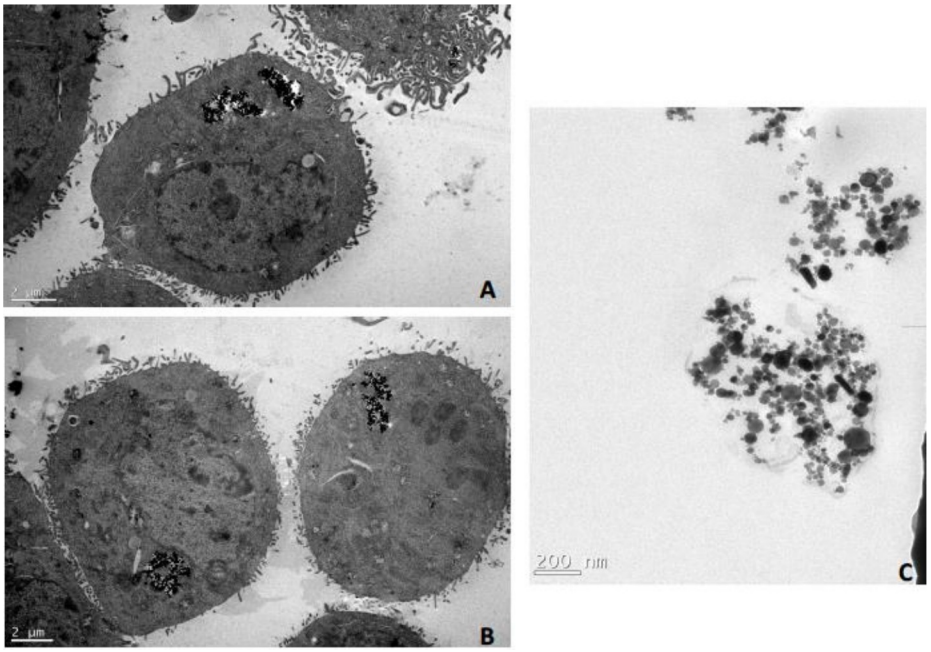

Fig 1. Transmission electron microscopy acquisition of DT66066 cells after 12 hours of incubation with NS. (A) and **(B)**: NS are incorporated into cell cytoplasm inside endocytic vacuoles; **C**: NS are released off the cell over 7–8 days into the surrounding extracellular matrix.

https://doi.org/10.1371/journal.pone.0209094.g001

For each condition, 14 to 18 spheroids were analyzed. The median diameter of non-treated spheroids (control) was 830.80 μm (SD = 70.89 μm). The average thickness was 300 to 350 μm. There was a significant and progressive reduction of spheroid diameter correlated with the increase of the cavitation index (Fig 5, Table 1, and Fig 6) ($p < 0.0001$).

EdU fluorescence quantification showed a significant reduction in cell proliferation with US intensity increment and with gemcitabine association (n = 8 or 9 spheroids per condition, $p<0.0001$) (Fig 7 and Fig 8), which was observed with all CI except CI 10 ($p = 0.99$).

Cells death was predominantly mediated by a necrosis mechanism, increased with US intensity increment as shown by Fig 9 and Fig 10 (n = 8 or 9 spheroids per condition, $p<0.0001$). There was a weak apoptotic effect, only significant for the condition "CI 14 + gemcitabine"(Fig 11).

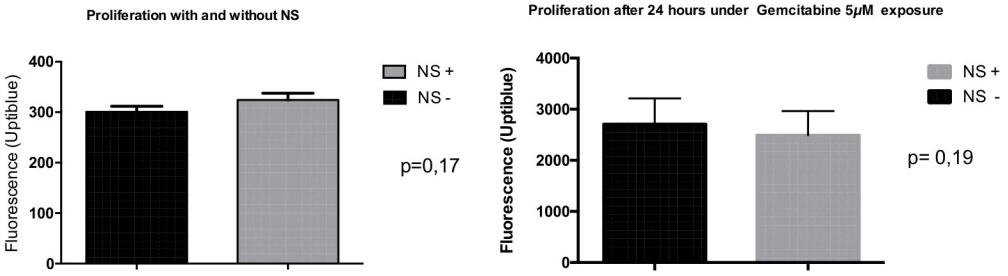

Fig 2. Cell proliferation and chemosensitivity to gemcitabine after incubation with NS (17–20 samples for each condition). Statistical analysis performed with Mann-Whitney test. NS impacted neither cell viability, proliferation, or chemosensitivity under gemcitabine exposure. *NS +: DT66066 cells incubated with NS; NS—: DT66066 cells without incubation with NS.*

https://doi.org/10.1371/journal.pone.0209094.g002

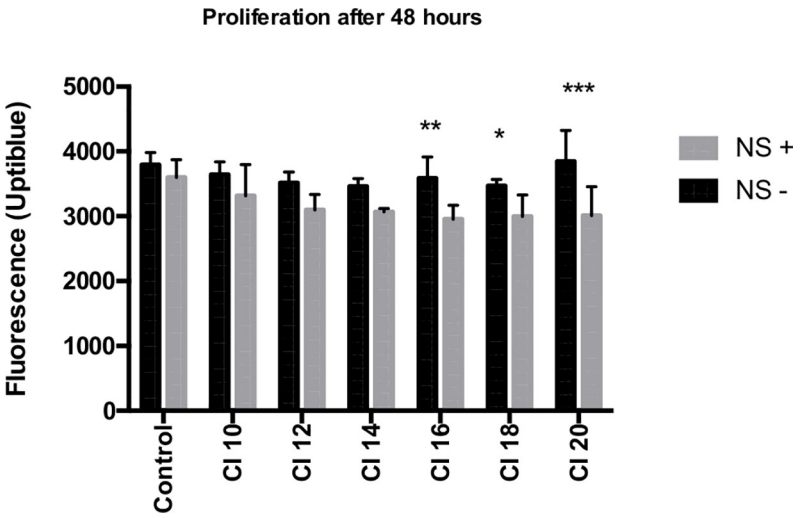

Fig 3. NS and cell sensitivity to US. 6 samples for each condition (a total of 84 samples). Statistical analysis performed with ANOVA test. *NS +: DT66066 cells incubated with NS; NS—: DT66066 cells without incubation with NS.*

https://doi.org/10.1371/journal.pone.0209094.g003

Discussion

Although the cytotoxicity of ultrasound, including inertial cavitation, has been described in various preclinical models for several decades [8,9], efforts to translate these effects in animal models have been sometimes disappointing [14,15]. This may result from an insufficient understanding of the optimal ultrasound regimen to be applied *in vivo* when the objective is either to kill cancer cells by mechanical means (while sparing healthy tissue) or to increase the penetration of drugs into malignant cells to potentiate chemotherapy. This is all the more important in the case of PDAC, where chemoresistance is especially overwhelming and the microenvironment is a particularly active player in the defense and promotion of cancer growth. We considered a good way to overcome some of these hurdles would be to proceed in a stepwise fashion, starting with a 3D model of PDAC. Three-dimensional cell culture models provide a more representative model of tumor growth and chemotherapy response than usual 2D models, because 3D models display spatial arrangement, biochemical and cellular heterogeneity that are more representative of *in vivo* tumor behavior. We started with a conventional, centrifugation-based spheroid model, then moved to a model based on magnetic nano-shuttle. To our knowledge, this work is the first to apply this method of 3D culture engineering to

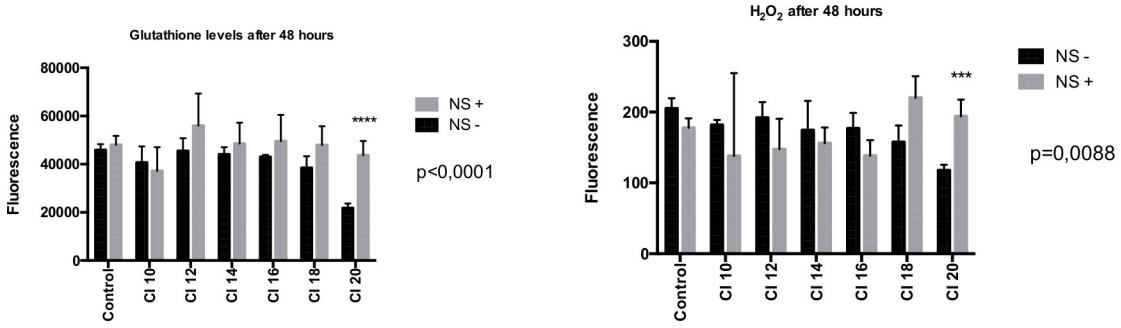

Fig 4. NS and oxidative stress. 6 samples for each condition (total of 84 samples). Statistical analyze performed with ANOVA test. *NS +: DT66066 cells incubated with NS; NS—: DT66066 cells without incubation with NS.*

https://doi.org/10.1371/journal.pone.0209094.g004

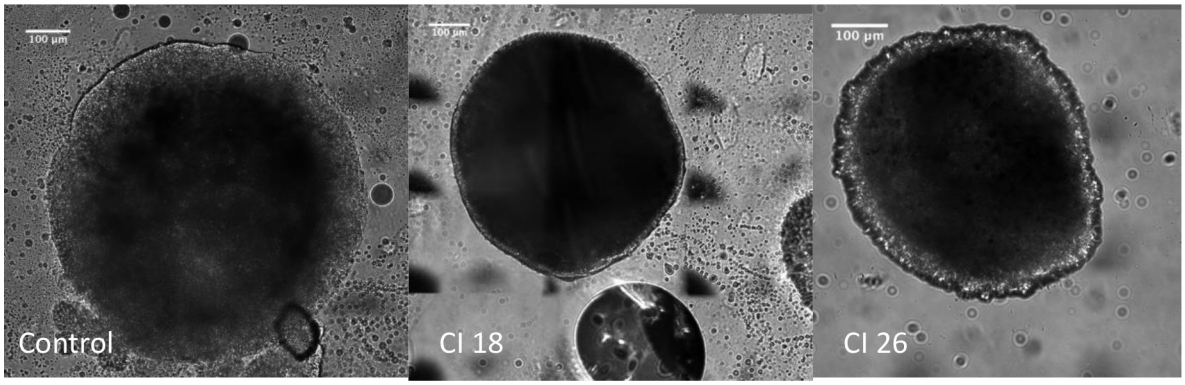

Fig 5. Examples of spheroids after inertial cavitation treatment. Images acquired using a straight confocal microscope, SPINNING DISK Leica DM6000 (Leica, Germany), 25X objective. *CI: Cavitation Index.*

https://doi.org/10.1371/journal.pone.0209094.g005

murine pancreatic adenocarcinoma cells. This 3D-nanoshuttle model provides excellent reproducibility and an easier handling of spheroids than a previous model we used, cultured in a more conventional manner [26–28]. This "conventional spheroid model", permitted to demonstrate some effects on tumor growth and synergism with chemotherapy on CAPAN-2-derived spheroids, but slower spheroid formation and more difficult handling for back and forth transfers between culture pits and ultrasonic exposures, which made it more difficult to analyze proliferation, necrosis and apoptosis [26]. A possible limitation of this work is the effect of the nanoparticles used to generate the 3D model. Indeed, although there was no impact on cell viability, proliferation, gemcitabine cell sensitivity, or oxidative stress, there was a significant reduction of cell proliferation for the highest cavitation index tested. As previously described, nanoparticles are eliminated from the spheroid at the eighth day of growth [16]. However, similar findings with both models in terms of growth impairment is a strong argument for their validity and against any bias induced by the magnetic nanoparticles in the nano-shuttle model. Our results reveal a therapeutic effect of inertial cavitation when combined with gemcitabine, but also when used alone. A decrease in size of the spheroids was the first significant observation, which was well correlated with increasing ultrasound intensity/index. In the same way, US treatment induced cell death whose predominant mechanism was necrosis. Different biophysical properties associated with inertial cavitation may explain these results: an increased cell membrane permeability, a modification of ionic homeostasis, the generation of reactive oxygen species (ROS), as well as ultrasound-specific thermal effects, any or a combination of which can lead to cell death [29–32].

Table 1. Size of spheroids at 24 hours after treatment.

	Control	Gem5 µM	CI10	CI10 + Gem5 µM	CI14	CI14 + Gem5 µM	CI18	CI18 + Gem5 µM	CI22	CI22 + Gem5 µM	CI26	CI26 + Gem5 µM
Diameter (mean in µm)	830.80	755.50	719.00	720.10	636.10	614.40	587.00	571.30	492.80	498.00	517.60	530.70
Standard deviation (m)	70.89	76.76	77.64	75.68	40.49	34.63	43.03	41.37	53.35	52.14	42.39	32.42
p value		0,02	<0.0001	<0.0001	<0.0001	<0.0001	<0.0001	<0.0001	<0.0001	<0.0001	<0.0001	<0.0001

14–18 spheroids for each condition. Statistical analysis performed with ANOVA.

CI: Cavitation Index; Gem 5 µM: Gemcitabine at a concentration of 5 µM

https://doi.org/10.1371/journal.pone.0209094.t001

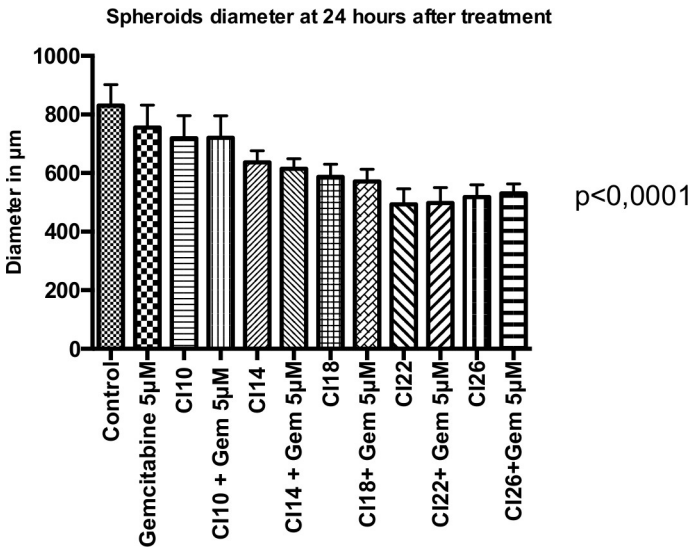

Fig 6. Size of spheroids at 24 hours after treatment. 14–18 spheroids for each condition. Statistical analysis performed with ANOVA test. *CI*: *Cavitation Index; Gem 5µM*: *Gemcitabine at a concentration of 5 µM*.

https://doi.org/10.1371/journal.pone.0209094.g006

Inertial cavitation also conferred a synergistic effect when combined with chemotherapy, which can be explained by several mechanisms: an increased cellular chemosensitivity, a modification of the drug's molecular structure leading to a more active or a more cytotoxic form, and an increased intra-cellular concentration of the chemotherapy. We observed a synergistic effect of inertial cavitation combined with gemcitabine at a concentration of 5 µM, but this was significant only for a cavitation index CI14, which is probably due to the fact that Gemcitabine is already cytotoxic at this concentration, thus explaining the limited synergism of the

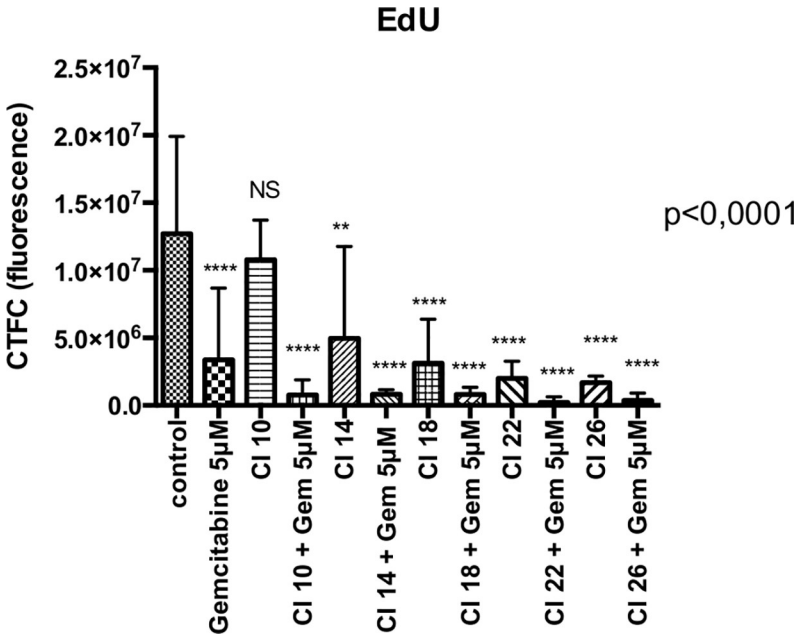

Fig 7. Cell proliferation quantified by EdU fluorescence. 8 or 9 spheroids per condition. Statistical analysis performed with ANOVA. *CI*: *Cavitation Index; Gem 5 µM*: *Gemcitabine at a concentration of 5 µM*

https://doi.org/10.1371/journal.pone.0209094.g007

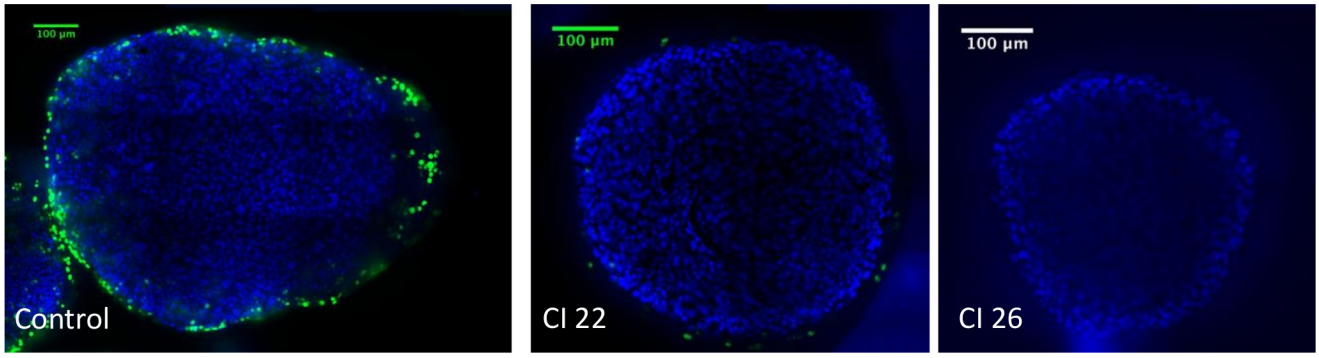

Fig 8. Examples of EdU plus DAPI fluorescence after inertial cavitation treatment. DAPI stains cell nuclei with a blue fluorescence. EdU stains phase S–entered cells with a green fluorescence. Images acquired using a straight confocal microscope, SPINNING DISK Leica DM6000 (Leica, Germany), 25X objective. *CI*: *Cavitation Index*.

https://doi.org/10.1371/journal.pone.0209094.g008

combination US + gemcitabine. Previous experiments carried out at a concentration of 20 μM showing a significant cytotoxicity on DT66066 cells in 2D cultures prompted us to reduce the concentration to 5 μM. Our results suggest that further reduction in the concentration of gemcitabine, in combination with inertial cavitation, would possibly exhibit more potent synergistic effects.

In this first step of the study of PDAC spheroids and inertial cavitation, the microenvironment tumor components were not included, although they are known to play a major role in

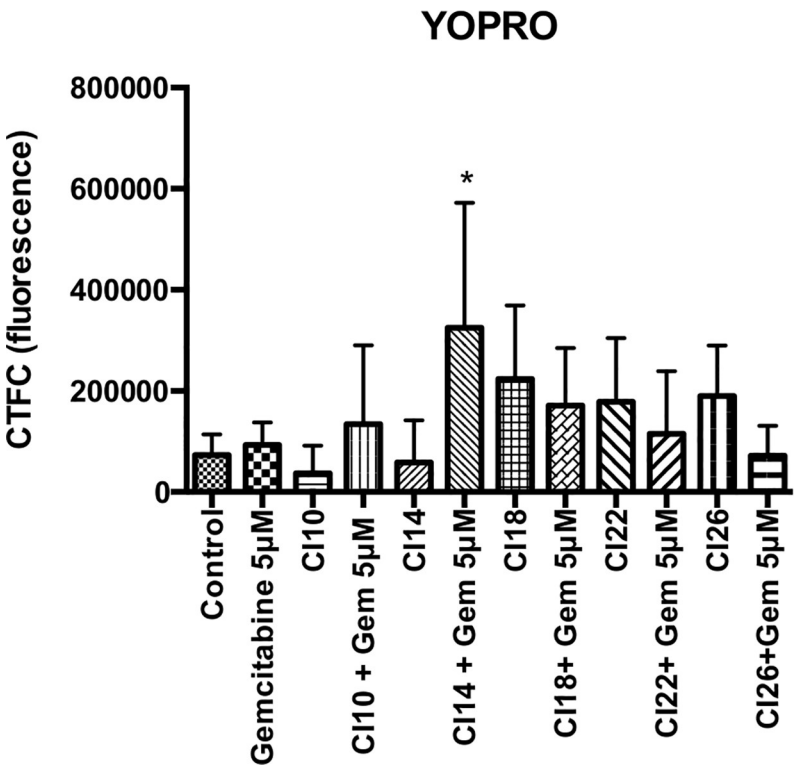

Fig 9. Cell apoptosis quantified by YO-PRO-1 fluorescence (without Propidium iodide fluorescence). 8 or 9 spheroids per condition. Statistical analysis performed with ANOVA. *CI*: *Cavitation Index; Gem 5 μM*: *Gemcitabine at a concentration of 5 μM*.

https://doi.org/10.1371/journal.pone.0209094.g009

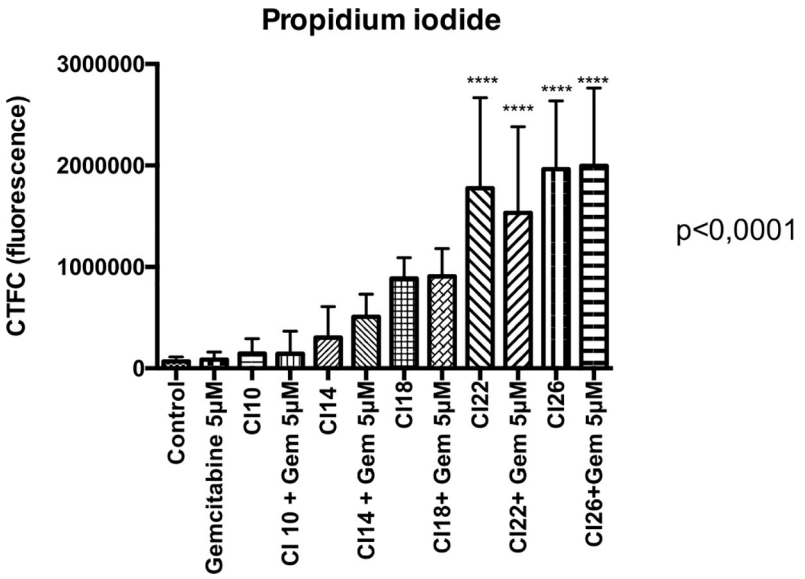

Fig 10. Propidium iodide fluorescence. 8 or 9 spheroids per condition. Statistical analysis performed with ANOVA. *CI: Cavitation Index; Gem 5 μM: Gemcitabine at a concentration of 5 μM.*

https://doi.org/10.1371/journal.pone.0209094.g010

the chemoresistance of pancreatic adenocarcinoma [33,34]. This is indeed an important limitation of this study. The next steps of this project will include the development of 3D co-culture models of pancreatic adenocarcinoma that incorporate the tumor microenvironment, and applying US treatment after eight days of spheroid growth in order to eliminate residual nanoparticles. Another important player in tumor development and drug distribution is vascularity, which is absent in spheroid models. Vascularized models may thus be necessary at a later stage, in the form of either organoids or genetically engineered animal models. However, the spheroid model appears to be particularly suitable for the reliable and reproducible analysis of short term cavitation-induced mechanical effects.

In conclusion, ultrasonic inertial cavitation applied in a 3D model of genetically engineered murine PDAC cell culture allowed a significant reduction of tumor growth, induced cells necrosis and synergized Gemcitabine under certain cavitation conditions. More investigations involving the development of a model including tumor microenvironment cells are needed in

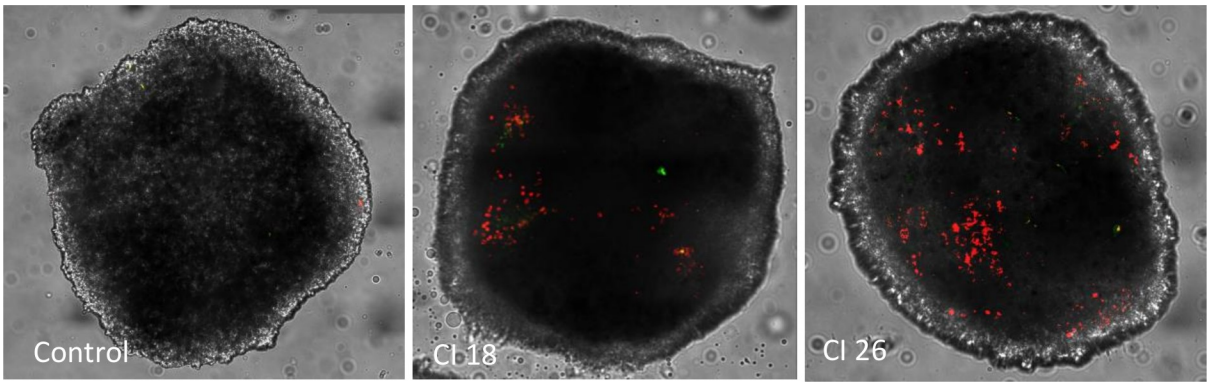

Fig 11. Examples of YO-PRO-1 fluorescence (green fluorescence) and Propidium iodide fluorescence (red fluorescence). Images acquired using a straight confocal microscope, SPINNING DISK Leica DM6000 (Leica, Germany), 25X objective. *CI: Cavitation Index.*

https://doi.org/10.1371/journal.pone.0209094.g011

the translational process towards a clinical application of ultrasonic cavitation to PDAC therapy.

Author Contributions

Conceptualization: Jean-Louis Mestas, Marine Camus, Frederic Prat.

Data curation: Einas Abou Ali, Marine Camus.

Formal analysis: Einas Abou Ali.

Funding acquisition: Einas Abou Ali.

Investigation: Einas Abou Ali, Benoit Bordacahar.

Methodology: Einas Abou Ali, Jean-Louis Mestas, Frederic Batteux, Marine Camus, Frederic Prat.

Project administration: Jean-Louis Mestas, Marine Camus, Frederic Prat.

Software: Einas Abou Ali, Jean-Louis Mestas.

Supervision: Jean-Louis Mestas, Frederic Batteux, Cyril Lafon, Marine Camus, Frederic Prat.

Validation: Einas Abou Ali, Jean-Louis Mestas, Frederic Batteux, Marine Camus, Frederic Prat.

Writing – original draft: Einas Abou Ali.

Writing – review & editing: Einas Abou Ali, Marine Camus, Frederic Prat.

References

1. Rahib L, Smith BD, Aizenberg R, Rosenzweig AB, Fleshman JM, Matrisian LM. Projecting cancer incidence and deaths to 2030: the unexpected burden of thyroid, liver, and pancreas cancers in the United States. Cancer Res. 2014 Jun 1; 74(11):2913–21. https://doi.org/10.1158/0008-5472.CAN-14-0155 PMID: 24840647
2. seer.cancer.gov.
3. Bosetti C, Bertuccio P, Negri E, La Vecchia C, Zeegers MP, Boffetta P. Pancreatic cancer: overview of descriptive epidemiology. Mol Carcinog. 2012 Jan; 51(1):3–13. https://doi.org/10.1002/mc.20785 PMID: 22162227
4. Von Hoff DD, Ervin T, Arena FP, Chiorean EG, Infante J, Moore M, et al. Increased survival in pancreatic cancer with nab-paclitaxel plus gemcitabine. N Engl J Med. 2013 Oct 31; 369(18):1691–703. https://doi.org/10.1056/NEJMoa1304369 PMID: 24131140
5. Conroy T, Desseigne F, Ychou M, Bouché O, Guimbaud R, Bécouarn Y, et al. FOLFIRINOX versus gemcitabine for metastatic pancreatic cancer. N Engl J Med. 2011 May 12; 364(19):1817–25. https://doi.org/10.1056/NEJMoa1011923 PMID: 21561347
6. Turrini O, Viret F, Moureau-Zabotto L, Guiramand J, Moutardier V, Lelong B, et al. Neoadjuvant chemoradiation and pancreaticoduodenectomy for initially locally advanced head pancreatic adenocarcinoma. Eur J Surg Oncol J Eur Soc Surg Oncol Br Assoc Surg Oncol. 2009 Dec; 35(12):1306–11.
7. Erkan M, Hausmann S, Michalski CW, Fingerle AA, Dobritz M, Kleeff J, et al. The role of stroma in pancreatic cancer: diagnostic and therapeutic implications. Nat Rev Gastroenterol Hepatol. 2012 Aug; 9 (8):454–67. https://doi.org/10.1038/nrgastro.2012.115 PMID: 22710569
8. Prat F, Chapelon JY, Chauffert B, Ponchon T, Cathignol D. Cytotoxic effects of acoustic cavitation on HT-29 cells and a rat peritoneal carcinomatosis in vitro. Cancer Res. 1991 Jun 1; 51(11):3024–9. PMID: 2032241
9. Prat F, Chapelon JY, el Fadil FA, Theillère Y, Ponchon T, Cathignol D. In vivo effects of cavitation alone or in combination with chemotherapy in a peritoneal carcinomatosis in the rat. Br J Cancer. 1993 Jul; 68 (1):13–7. PMID: 8318402
10. Carpentier A, Canney M, Vignot A, Reina V, Beccaria K, Horodyckid C, et al. Clinical trial of blood-brain barrier disruption by pulsed ultrasound. Sci Transl Med. 2016 Jun 15; 8(343):343re2. https://doi.org/10.1126/scitranslmed.aaf6086 PMID: 27306666

11. Horodyckid C, Canney M, Vignot A, Boisgard R, Drier A, Huberfeld G, et al. Safe long-term repeated disruption of the blood-brain barrier using an implantable ultrasound device: a multiparametric study in a primate model. J Neurosurg. 2017 Apr; 126(4):1351–61. https://doi.org/10.3171/2016.3.JNS151635 PMID: 27285538

12. Brennen CE. Cavitation in medicine. Interface Focus [Internet]. 2015 Oct 6 [cited 2017 Sep 2]; 5(5). Available from: http://www.ncbi.nlm.nih.gov/pmc/articles/PMC4549847/

13. Kotopoulis S, Stigen E, Popa M, Safont MM, Healey A, Kvåle S, et al. Sonoporation with Acoustic Cluster Therapy (ACT®) induces transient tumour volume reduction in a subcutaneous xenograft model of pancreatic ductal adenocarcinoma. J Controlled Release. 2017 Jan 10; 245:70–80.

14. Li T, Wang Y-N, Khokhlova TD, D'Andrea S, Starr F, Chen H, et al. Pulsed High-Intensity Focused Ultrasound Enhances Delivery of Doxorubicin in a Preclinical Model of Pancreatic Cancer. Cancer Res. 2015 15; 75(18):3738–46. https://doi.org/10.1158/0008-5472.CAN-15-0296 PMID: 26216548

15. Huang P, Zhang Y, Chen J, Shentu W, Sun Y, Yang Z, et al. Enhanced antitumor efficacy of ultrasonic cavitation with up-sized microbubbles in pancreatic cancer. Oncotarget. 2015 Aug 21; 6(24):20241–51. https://doi.org/10.18632/oncotarget.4048 PMID: 26036312

16. Haisler WL, Timm DM, Gage JA, Tseng H, Killian TC, Souza GR. Three-dimensional cell culturing by magnetic levitation. Nat Protoc. 2013 Oct; 8(10):1940–9. https://doi.org/10.1038/nprot.2013.125 PMID: 24030442

17. Souza GR, Molina JR, Raphael RM, Ozawa MG, Stark DJ, Levin CS, et al. Three-dimensional tissue culture based on magnetic cell levitation. Nat Nanotechnol. 2010 Apr; 5(4):291–6. https://doi.org/10.1038/nnano.2010.23 PMID: 20228788

18. Westphalen CB, Olive KP. Genetically engineered mouse models of pancreatic cancer. Cancer J Sudbury Mass. 2012 Dec; 18(6):502–10.

19. Lee JW, Komar CA, Bengsch F, Graham K, Beatty GL. Genetically Engineered Mouse Models of Pancreatic Cancer: The KPC Model (LSL-Kras(G12D/+);LSL-Trp53(R172H/+);Pdx-1-Cre), Its Variants, and Their Application in Immuno-oncology Drug Discovery. Curr Protoc Pharmacol. 2016 Jun 1; 73:14.39.1–14.39.20.

20. Tseng H, Gage JA, Raphael RM, Moore RH, Killian TC, Grande-Allen KJ, et al. Assembly of a three-dimensional multitype bronchiole coculture model using magnetic levitation. Tissue Eng Part C Methods. 2013 Sep; 19(9):665–75. https://doi.org/10.1089/ten.TEC.2012.0157 PMID: 23301612

21. Daquinag AC, Souza GR, Kolonin MG. Adipose tissue engineering in three-dimensional levitation tissue culture system based on magnetic nanoparticles. Tissue Eng Part C Methods. 2013 May; 19(5):336–44. https://doi.org/10.1089/ten.TEC.2012.0198 PMID: 23017116

22. Tseng H, Balaoing LR, Grigoryan B, Raphael RM, Killian TC, Souza GR, et al. A three-dimensional co-culture model of the aortic valve using magnetic levitation. Acta Biomater. 2014 Jan; 10(1):173–82. https://doi.org/10.1016/j.actbio.2013.09.003 PMID: 24036238

23. Chettab K, Mestas J-L, Lafond M, Saadna DE, Lafon C, Dumontet C. Doxorubicin Delivery into Tumor Cells by Stable Cavitation without Contrast Agents. Mol Pharm. 2017 06; 14(2):441–7. https://doi.org/10.1021/acs.molpharmaceut.6b00880 PMID: 28107023

24. McCloy RA, Rogers S, Caldon CE, Lorca T, Castro A, Burgess A. Partial inhibition of Cdk1 in G 2 phase overrides the SAC and decouples mitotic events. Cell Cycle Georget Tex. 2014; 13(9):1400–12.

25. Burgess A, Vigneron S, Brioudes E, Labbé J-C, Lorca T, Castro A. Loss of human Greatwall results in G2 arrest and multiple mitotic defects due to deregulation of the cyclin B-Cdc2/PP2A balance. Proc Natl Acad Sci U S A. 2010 Jul 13; 107(28):12564–9. https://doi.org/10.1073/pnas.0914191107 PMID: 20538976

26. Benoit Bordacahar, Marine Camus, Einas Abou Ali, Jean Louis Mestas, Maxime Lafond, Ivan Suarez, aurélie gomes, valérie lobjois, Frédéric Batteux, Cyril Lafon, Frédéric Prat. EFFECT OF ACOUSTIC CAVITATION ON A THREE-DIMENSIONAL CULTURE MODEL OF PANCREATIC ADENOCARCINOMA. Abstract UEGW 2017, United European Gastroenterology Journal 2017; 5 (Supplement 1) presented at;

27. Dufau I, Frongia C, Sicard F, Dedieu L, Cordelier P, Ausseil F, et al. Multicellular tumor spheroid model to evaluate spatio-temporal dynamics effect of chemotherapeutics: application to the gemcitabine/CHK1 inhibitor combination in pancreatic cancer. BMC Cancer. 2012 Jan 13; 12(1):15.

28. Laurent J, Frongia C, Cazales M, Mondesert O, Ducommun B, Lobjois V. Multicellular tumor spheroid models to explore cell cycle checkpoints in 3D. BMC Cancer. 2013 Feb 8; 13(1):73.

29. Rosenthal I, Sostaric JZ, Riesz P. Sonodynamic therapy—a review of the synergistic effects of drugs and ultrasound. Ultrason Sonochem. 2004 Sep; 11(6):349–63. https://doi.org/10.1016/j.ultsonch.2004.03.004 PMID: 15302020

30. Nomikou N, McHale AP. Exploiting ultrasound-mediated effects in delivering targeted, site-specific cancer therapy. Cancer Lett. 2010 Oct 28; 296(2):133–43. https://doi.org/10.1016/j.canlet.2010.06.002 PMID: 20598800

31. Duco W, Grosso V, Zaccari D, Soltermann AT. Generation of ROS mediated by mechanical waves (ultrasound) and its possible applications. Methods. 2016 Oct 15; 109:141–8. https://doi.org/10.1016/j.ymeth.2016.07.015 PMID: 27542338

32. Ebbini ES, ter Haar G. Ultrasound-guided therapeutic focused ultrasound: current status and future directions. Int J Hyperth Off J Eur Soc Hyperthermic Oncol North Am Hyperth Group. 2015 Mar; 31 (2):77–89.

33. Hessmann E, Patzak MS, Klein L, Chen N, Kari V, Ramu I, et al. Fibroblast drug scavenging increases intratumoural gemcitabine accumulation in murine pancreas cancer. Gut. 2017 Jan 10;

34. Liu Y, Li F, Gao F, Xing L, Qin P, Liang X, et al. Periostin promotes the chemotherapy resistance to gemcitabine in pancreatic cancer. Tumour Biol J Int Soc Oncodevelopmental Biol Med. 2016 Nov; 37 (11):15283–91.